

NOAA Technical Memorandum NWS WR-127

DEVELOPMENT OF A PROBABILITY EQUATION FOR WINTER-TYPE
PRECIPITATION PATTERNS IN GREAT FALLS, MONTANA

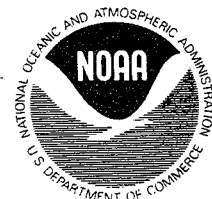
Kenneth B. Mielke

National Weather Service Forecast Office
Great Falls, Montana
March 1978

UNITED STATES
DEPARTMENT OF COMMERCE
Juanita M. Kreps, Secretary

/ NATIONAL OCEANIC AND
ATMOSPHERIC ADMINISTRATION /
Richard Frank,
Administrator

/ NATIONAL WEATHER
SERVICE /
George P. Cressman, Director



CONTENTS

	<u>Page</u>
Abstract	1
I. Introduction	1
II. Data	2
III. Analysis	3
IV. Comparison of MOS and Derived Equation	6
V. Conclusion	6
VI. Acknowledgments	7
References	7

FIGURES AND TABLES

	<u>Page</u>
Figure 1. Area considered in this precipitation study . . .	8
Figure 2. Measurable precipitation probability as a function of the GTF 500-mb contour crossing at 145W and 130W	9
Figure 3. Measurable precipitation probability as a function of the ZU-BOI sea-level pressure difference and the difference between the 500-mb GTF contour crossing through 145W or 130W and the 120W contour crossing value in degrees latitude	9
Figure 4. Probability of measurable precipitation as a function of the isoplethed probability categories of Figure 2 versus the probability categories of Figure 3	10
Figure 5. Histogram displaying the range of Y values from the linear regression	11
Table 1. Measurable precipitation probability at GTF as a function of the GTF 500-mb contour crossing at the 145W and 130W meridians . . .	12
Table 2. A breakdown of all measurable precipitation cases in this study as a function of the highest latitudinal crossing of the GTF 500-mb contour at key longitude meridians . .	13
Table 3. A comparison of MOS and derived-equation first-period probabilities	14
Table 4. A comparison of MOS and derived-equation first-period probabilities during a relatively dry period in October 1977	15
Table 5. A comparison of MOS and derived equation 1st, 2nd, and 3rd 12-hour period probabilities during a period in December 1977	16

DEVELOPMENT OF A PROBABILITY EQUATION FOR WINTER-TYPE
PRECIPITATION PATTERNS IN GREAT FALLS, MONTANA

Kenneth B. Mielke
National Weather Service Forecast Office
Great Falls, Montana

ABSTRACT. Four parameters known to be reliable predictors of winter-type precipitation patterns (Oct-Mar) at Great Falls, Montana, are analyzed independently and then integrated into a probability of measurable precipitation equation. Five hundred fifty-one (551) cases are studied involving surface and upper-air data. The occurrence of precipitation at Great Falls, Montana, is strongly dependent upon the development of upslope conditions along the east slopes of the Rocky Mountains in Montana. Successive graphical regression analysis is first used to show the strength of the four parameters collectively. A probability equation is then developed by a linear regression program. The derived equation is compared with the Model Output Statistics and is shown to have practical value as a forecast tool.

I. INTRODUCTION

Winter-type precipitation and storms in Montana have always been a focal point of discussion and research among the forecasters at the Weather Service Forecast Office (WSFO) at Great Falls, MT. Their frequent occurrence and rapid development generated various schemes, indices, and rules of thumb to aid the forecaster in predicting onset, duration and intensity of these systems. This report develops another such forecast tool.

Harding (1972) discussed in detail the ridge-trough relationships in the Gulf of Alaska and the antecedent development of upslope/downslope conditions along the east slopes of the Rockies in Montana. Downslope in this region is characterized by southwesterly winds while upslope winds have a northerly component. Basically, two index systems were devised by Harding (1972). The first was a comparison of sea-level-pressure relationships among the Whitecourt (ZU), Alta; Juneau (JNU), AK; Annette (ANN), AK; Boise (BOI), ID; and Great Falls (GTF), MT, stations (Figure 1). Rising or higher pressures in Alaska which translate downstream along the lee slopes of the Canadian Rockies are easily monitored by graphing these representative stations and such values/gradients precede the development of upslope wind flow along the lee slopes of the Rockies in Montana. Conversely, falling or lower pressures at the northern-most stations are a reflection of lee trough development east of the Canadian Rockies and eventual downslope conditions east of the divide in Montana. The intensification or movement of a low-pressure system into the Gulf of Alaska is usually a

prerequisite for this situation. Analysis by Harding (1972) of several case histories based on these surface-pressure relationships yielded a timing scheme for Arctic and Pacific Northern* fronts in Montana.

The second index system employs upper-air data, specifically, latitudinal crossing (in degrees) of the GTF 500-mb contour through the 120°W , 130°W , and 145°W longitude meridians (Figure 1). This index becomes positive (for measurable precipitation) if the value of the latitudinal crossings at 130°W and/or 145°W are greater than the 120°W contour crossing value. Increasingly higher values of contour crossings at the 130°W and 145°W meridians indicate upper-ridge development over the Gulf of Alaska. This situation normally leads to the filling of the lee side trough and possible upslope development in Montana. In some ways, this index system could be compared with the 500-mb map-type system (Augulis 1970).

The absolute values, gradients and interaction of these indices are used to determine the onset and intensity of upslope/downslope situations along the east slopes of the Rockies in Montana; the key to winter-type precipitation forecasts. As shown convincingly by Harding (1972), less than 10% of measurable precipitation at GTF occurs during downslope conditions. Often, one index will remain negative while the other index becomes positive. For example, a positive upper-air index (short-wave trough approaching) may exist, yet the current surface index (and its prognosis) indicates downslope along the lee slopes of the Rockies. While precipitation may develop west of the divide in Montana, it could become quite spotty or never develop along the east slopes of the Rockies if sufficient downslope winds persist. The purpose of this study is to combine these parameters in an effort to develop a probability equation for winter-type precipitation in Great Falls.

II. DATA

Data were obtained from index graphs stored at the GTF WSFO for the 6-month period October-March from 1974 through December 1976. Surface pressure graphs are normally plotted at 3-hour intervals while the 500-mb data are plotted at 12-hour intervals. Twelve-hour precipitation amounts are plotted on these graphs also. Graphical index values were extracted which resulted in 551 case histories involving 95 measurable precipitation events.

*A Pacific Northern front, as defined by the Great Falls forecasters, is one in which the winds shift to the northwest after passage, giving 3 to 12 hours of upslope conditions. Its air mass is typically cool and unstable, originating from the Gulf of Alaska. An approaching front is defined as a Pacific Northern if the sea-level pressure at SHIP PAPA (C7P) exceeds the GTF sea-level pressure.

III. ANALYSIS

The graphical representation presented several possible combinations of indicators that could be used in a probability scheme. Four parameters were chosen which were known to be individually strong indicators of measurable precipitation at Great Falls.

The first parameter was the difference between sea-level pressures at ZU and BOI. This difference reflects upslope conditions along the lee slopes of the Rockies when ZU sea-level pressure is greater than that of BOI and downslope when the BOI-sea level pressure is higher. This difference is defined as positive when $ZU-BOI > 0$. The BOI sea-level pressure was used instead of the GTF sea-level pressure since a strong basin high-pressure area, usually centered near BOI, can offset pressure rises along the lee slopes of the Canadian Rockies. For example, ZU sea-level pressure may exceed the GTF value, however, BOI sea-level pressure may exceed both the GTF and ZU values inhibiting upslope development along the lee slopes in Montana. The more positive the ZU-BOI difference becomes, the greater upslope development is expected along the east slopes of the Rockies in southern Alberta and Montana. Conversely, increasingly negative values of this difference indicate strengthening downslope conditions in this region. Considering all cases in this study, the ZU-BOI difference was greater than zero 143 times and 62 cases of measurable precipitation (.01 of an inch or more) occurred in the following 12-hour period. This parameter alone, then, gives a 43% probability.

The remaining three parameters involved the GTF 500-mb contour latitude crossing at $120^{\circ}W$, $130^{\circ}W$, and $145^{\circ}W$ longitude. As stated earlier, increasing latitude of the contour crossing at $130^{\circ}W$ and $145^{\circ}W$ are indicative of ridge development in the Gulf of Alaska. This is a necessary but not a sufficient prerequisite for expecting the lee side trough in Alberta to fill. Conversely, lowering values of these crossings correlate with lee trough development or enhancement east of the Rockies.

Table 1 illustrates the predictive qualities of these two parameters for measurable precipitation. Note, when the contour crosses $145^{\circ}W$ at or above $65^{\circ}N$, the probability of precipitation for the following 12-hour period is 66%. As the contour crossings are divided into 5° latitudinal increments, the probabilities decrease dramatically as the contour crossing value decreases. Table 1 also gives the same breakdown for $130^{\circ}W$ meridian crossings. The values are very nearly the same. In Table 2, a comparison of the three contour-crossing values is given for the 95 measurable precipitation cases only. This table emphasizes the importance of 500-mb ridging near $145^{\circ}W$ for precipitation events in Great Falls. In 60% of the measurable precipitation cases, the $145^{\circ}W$ contour crossing equaled or exceeded the values at $120^{\circ}W$ and $130^{\circ}W$. The $120^{\circ}W$ meridian has not been analyzed in as much detail as the other two meridians because of its proximity to GTF, which would diminish its predictive quality. Instead, the contour crossing value at $120^{\circ}W$ is utilized as a standard to measure the amplitudes of the $130^{\circ}W$ and $145^{\circ}W$

contour values, as will be discussed later. Based on Table 1, therefore, the values of the 130°W and 145°W contour crossings are used as the second and third parameters.

The final parameter involved the difference between the 145°W or 130°W contour crossing values and the 120°W value. This difference is defined as positive when the 145°W/130°W values exceed the 120°W value. The higher of the latitude crossing values at the 145°W and 130°W meridians is used and this difference comprises the fourth parameter. This difference measures the amplitude of the 500-mb wavelength upstream from GTF. For example, a large positive value of the (145°W/130°W-120°W) difference would indicate a high amplitude ridge in the Gulf of Alaska and a trough in the western United States. The magnitude of this amplitude is a measure of upslope intensity. Large positive differences can also be attained when a sharp short-wave 500-mb trough tracks into the Pacific Northwest. In this sense, the difference can also be thought of as a measure of curvature or vorticity advection into Montana. Either of these situations is conducive to upslope development. Of the 551 cases in this study, the (145°W/130°W-120°W) difference was greater than zero 264 times. Of these 264 cases, 85 involved measurable precipitation for a 32% probability in a 12-hour period. With the strength of the 4 parameters now established on an individual basis, a combination of these predictors into a single probability forecast value seemed appropriate.

The successive graphical regression method shown by Panofsky (1965) was first employed to determine how much variance could be reduced by combining the parameters. First, the 500-mb latitudinal crossing, in degrees, of the GTF contour at 145°W was plotted against the crossing at 130°W (Figure 2). Of course, the linear relationship between these two parameters is necessarily strong, as shown by the best-fit line. This graph was accomplished, however, to obtain isopleths of probabilities as shown.

In the second graph shown in Figure 3, the (ZU-BOI) sea-level pressure difference was plotted against the greater of the (145°W/130°W-120°W) contour differences. The scatter about the best-fit curve was greater; however, measurable probability categories were easily delineated. The best probability of measurable precipitation occurred in the quadrant where both values were positive, while the lowest probability centered in the negative quadrant. Next a third graph was constructed as shown in Figure 4 using the probability categories from Figure 3 as the ordinates and those from Figure 2 as the abscissa. Again, the cases were plotted and values isoplethed, resulting in 5 well-defined probability categories. This method graphically reduced the variance of the probability forecast.

In practice, the use of three graphs is often cumbersome; therefore, a mathematical expression is more desirable. A linear regression equation program was available on the Statistical Programs cassette of the Wang Computer. This equation had the form,

$$Y = A_1 X_1 + A_2 X_2 + A_3 X_3.$$

Since only three independent variables were allowed, one of the four forecast parameters had to be eliminated or two had to be combined. From the above discussion and Figure 2, it is evident that the 500-mb crossing value, in degrees latitude, at 130°W and 145°W correlated quite well. Therefore, in each case, these two parameters were added to form a single variable. Y is the dichotomous dependent variable having the value 1.0 for measurable precipitation and 0.0 for trace or none. Substitution of these variables into the program yielded the following equation:

$$Y = .01251X_1 + .00132X_2 + .02361X_3$$

where

X_1 = (ZU-BOI) sea-level pressure in millibars

X_2 = The sum, in degrees latitude, of the GTF 500-mb contour crossing at 145°W and 130°W (Ex., 50° + 45° = 95°)

X_3 = The difference of the 120°W GTF 500-mb contour crossing value, in degrees latitude, from the value at 130°W or 145°W. The larger of the two values at 145°W and 130°W is used.

The magnitudes of X_1 and X_3 are 10^1 while the magnitude of X_2 is 10^2 . Therefore, each of the three terms in the equation has a magnitude of approximately 10^{-1} .

The dependent variable, Y (probability) was then plotted onto a histogram in order to determine appropriate class intervals of probability. This procedure revealed six well-defined probability classes, as shown in Figure 5, ranging from 2% to 85%. Class sizes and intervals were not uniform due to the strong bias in the sample towards no precipitation. Also, shown in Figure 5 are the occurrences of trace events and the probabilities of a trace or more precipitation in each class interval. Over a third of all precipitation events in this study involved a trace.

The classes in Figure 5 were then rounded down to the nearest 10% which yielded six probability categories of 2%, 10%, 20%, 40%, 60% and 80%. These values and their limits were incorporated into a computer program. By inputting the BOI and ZU sea-level pressures and the 120°W, 130°W, and 145°W GTF 500-mb contour crossings, the appropriate probabilities of measurable and trace or more precipitation during the following 12-hour period are printed out. By using the LFM or PE upper air and surface progs, four 12-hour probabilities of precipitation can be obtained. Actual data are used for the 1st 12-hour forecast. In some cases, mixing of the data from the progs yields a better solution. The LFM surface progs frequently forecast too much of a downslope gradient from southern Alberta into Montana east of the Rockies. If this error is large, it can offset the upper-air parameters and low probabilities of precipitation result. The speed and height changes of the LFM upper-air progs, however, are generally preferred over the PE. Therefore, in some cases, the use of the LFM upper-air data mixed with the PE surface progs yields a desirable compromise.

IV. COMPARISON OF MOS AND DERIVED EQUATION

The Model Output Statistics PoPs were compared against the equation derived PoPs during the period 3-11 January 1977. The long-wave pattern consisted of a 500-mb ridge near 140°W and a trough over the eastern United States. Short-wave troughs tracked down the east side of the ridge across Montana into the long-wave trough resulting in several periods of precipitation at Great Falls. In Table 3 is a comparison of 17 consecutive 12-hour periods, for which data were available. In this example, actual data were substituted into the derived equation to determine PoPs. During this period, the equation PoPs fared quite well, scoring a 37% improvement over MOS, based on the Brier Score. In Table 4, a similar comparison is shown during a dry period from 22-31 October 1977. Again, actual data were substituted into the derived equation to determine the PoPs. In 20 consecutive 12-hour periods, improvement over MOS Pops was 86%.

Shown in Table 5 is a comparison of the 1st, 2nd and 3rd period MOS and the derived-equation forecasts during a 12-day period in December 1977. In this example, the derived-equation probabilities are obtained from the 12-, 24- and 36-hour LFM surface and upper-air progs, rather than from the actual observations. The derived equation PoPs displayed an improvement over MOS PoPs of 9.3% in the 1st period, 7.6% in the second and 18.4% in the 3rd. Overall, the improvement over MOS was 11.6%. Using the LFM progs as input into the derived equation is a more realistic approach to the use of this product in operational forecasting. This approach, however, assumes a perfect prog, which isn't always the case. Therefore, the results are not only a measure of the derived equation's accuracy, but also of the prog itself.

V. CONCLUSION

The predictive characteristics of the four parameters analyzed in this study have been qualitatively known to Great Falls WSFO forecasters for many years. This study attempted to combine and quantify these predictors into a useful single forecast tool. An advantage of the derived probability equation is its flexibility. Data can be entered into the program from either the LFM or PE surface and upper-air progs, from actual observations or data can be mixed from the progs.

The derived probability equation also serves as an objective comparison to the MOS probability values. The probability equation obtained in this study is, of course, biased towards ridge development in the Gulf of Alaska and upslope flow east of the Rockies when measurable precipitation is expected. The MOS equations contain more parameters, however, and will likely yield better results in some cases, such as warm-air advection precipitation. Nevertheless, as shown in Table 3, during classical winter-type precipitation patterns, the derived probability equation can be expected to give quite good results.

VI. ACKNOWLEDGMENTS

I would like to express a sincere thanks to Mr. Warren G. Harding, Lead Forecaster at the Great Falls WSFO, for the many inspiring discussions on precipitation forecasting at Great Falls and for the use of the graphical data that made this research project possible. I would also like to thank Dr. Sandy MacDonald and Mr. Leonard Snellman at the Scientific Services Division for their helpful comments and suggestions.

REFERENCES

Harding, Warren G., 1972: Forecasting Arctic Outbreaks into the Great Falls Area. Manuscript at Great Falls, MT, WSFO. Presented at National AMS Conference, Portland, OR, 1972.

Panofsky, Hans A. and Glen W. Brier, 1965: Some Applications of Statistics to Meteorology, pp. 180-183.

Augulis, Richard P., 1970: Precipitation Probabilities in the Western Region Associated with 500-MB Map Types. WBTM Technical Memorandum, WBTM WR 45/1-4, National Oceanic and Atmospheric Administration, U.S. Department of Commerce, National Weather Service Western Region.

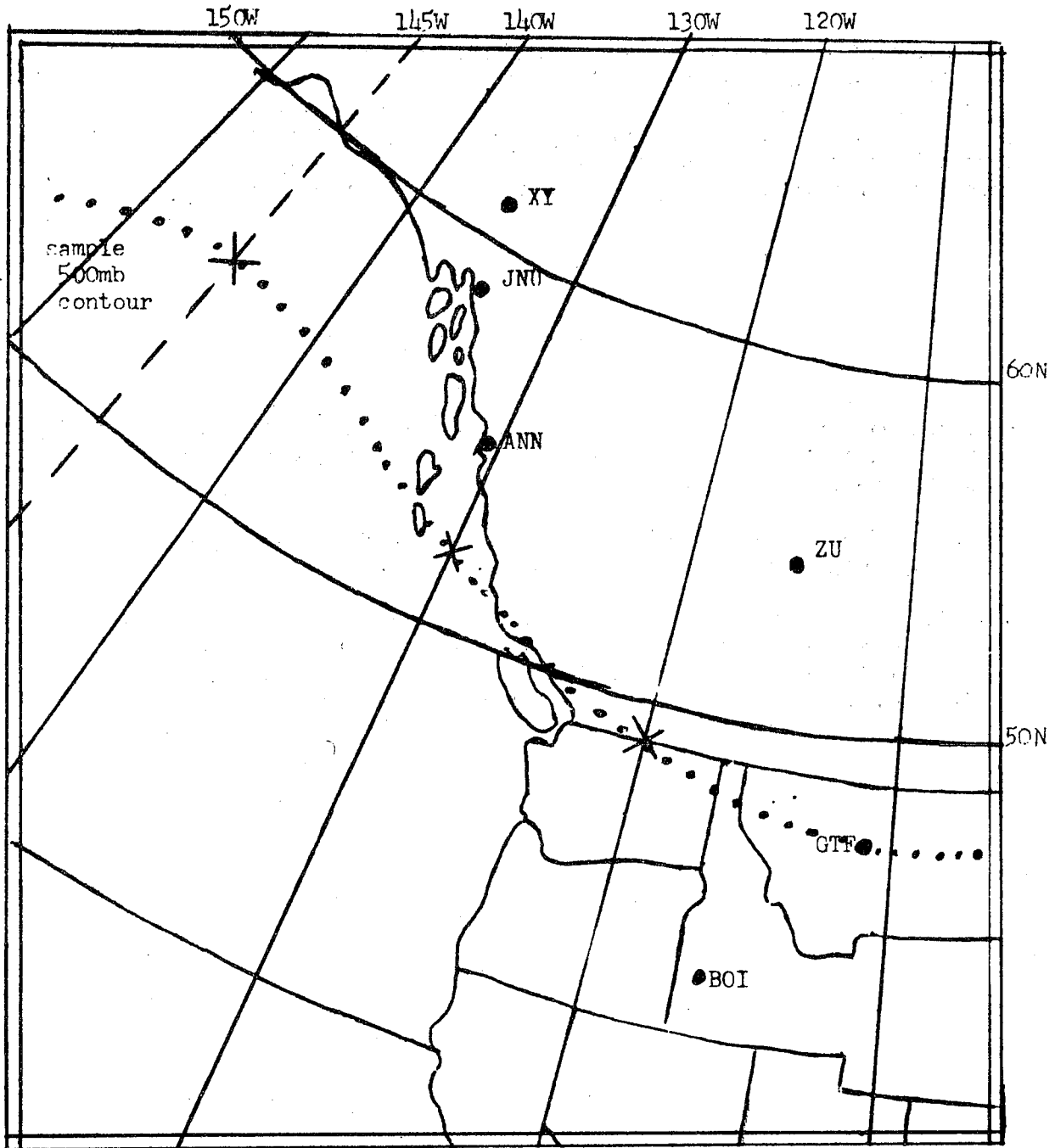


Figure 1. Area considered in this precipitation study. Dotted lines indicate a hypothetical 500-mb contour through GTF with intersections at key meridians marked.

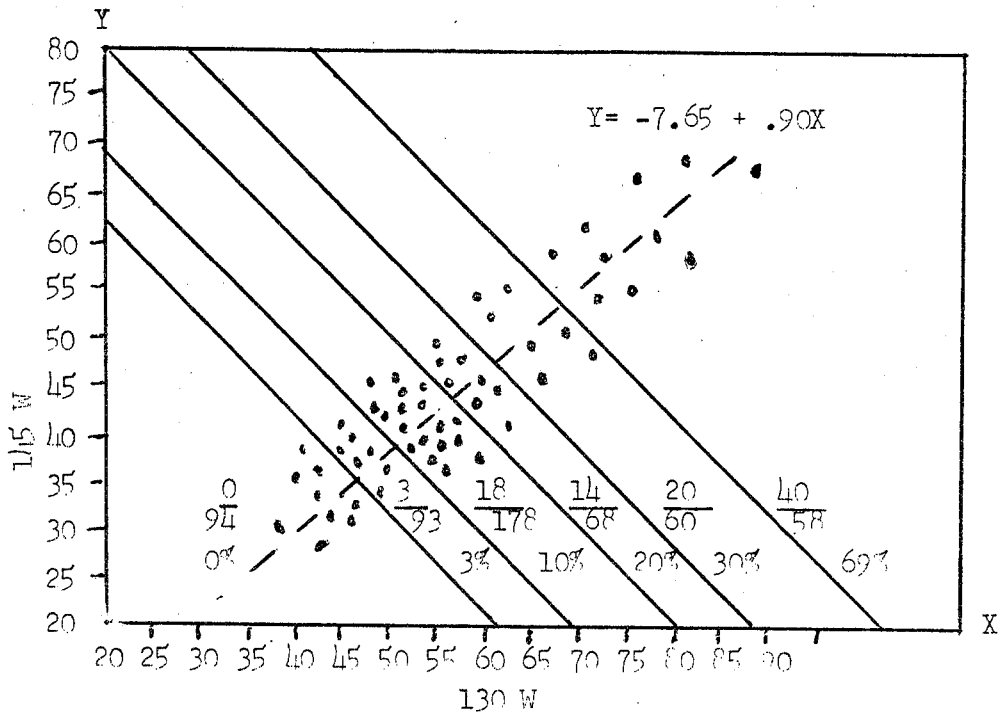


Figure 2. Measurable precipitation probability as a function of the GTF 500-mb contour crossing at 145W and 130W. Best-fit equation to data also given. A fraction of the data points are plotted to illustrate a representative distribution.

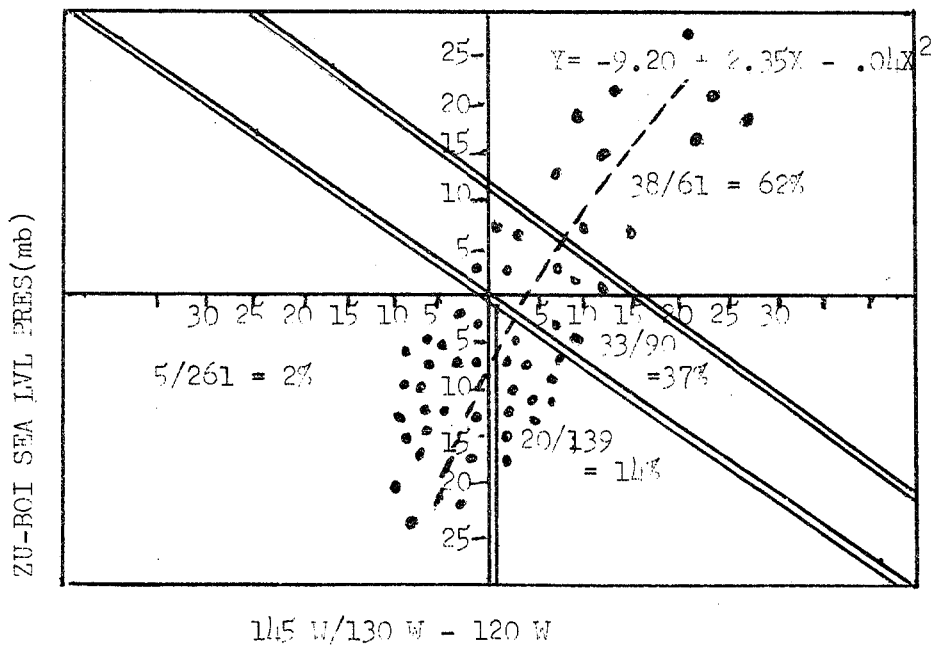


Figure 3. Measurable precipitation probability as a function of the ZU-B01 sea-level pressure difference and the difference between the 500-mb GTF contour crossing through 145W or 130W and the 120W contour crossing value in degrees latitude. The contour crossing value which is the higher, in degrees latitude, of the 130W or 145W meridians is used. A fraction of the data points are plotted to illustrate a representative distribution.

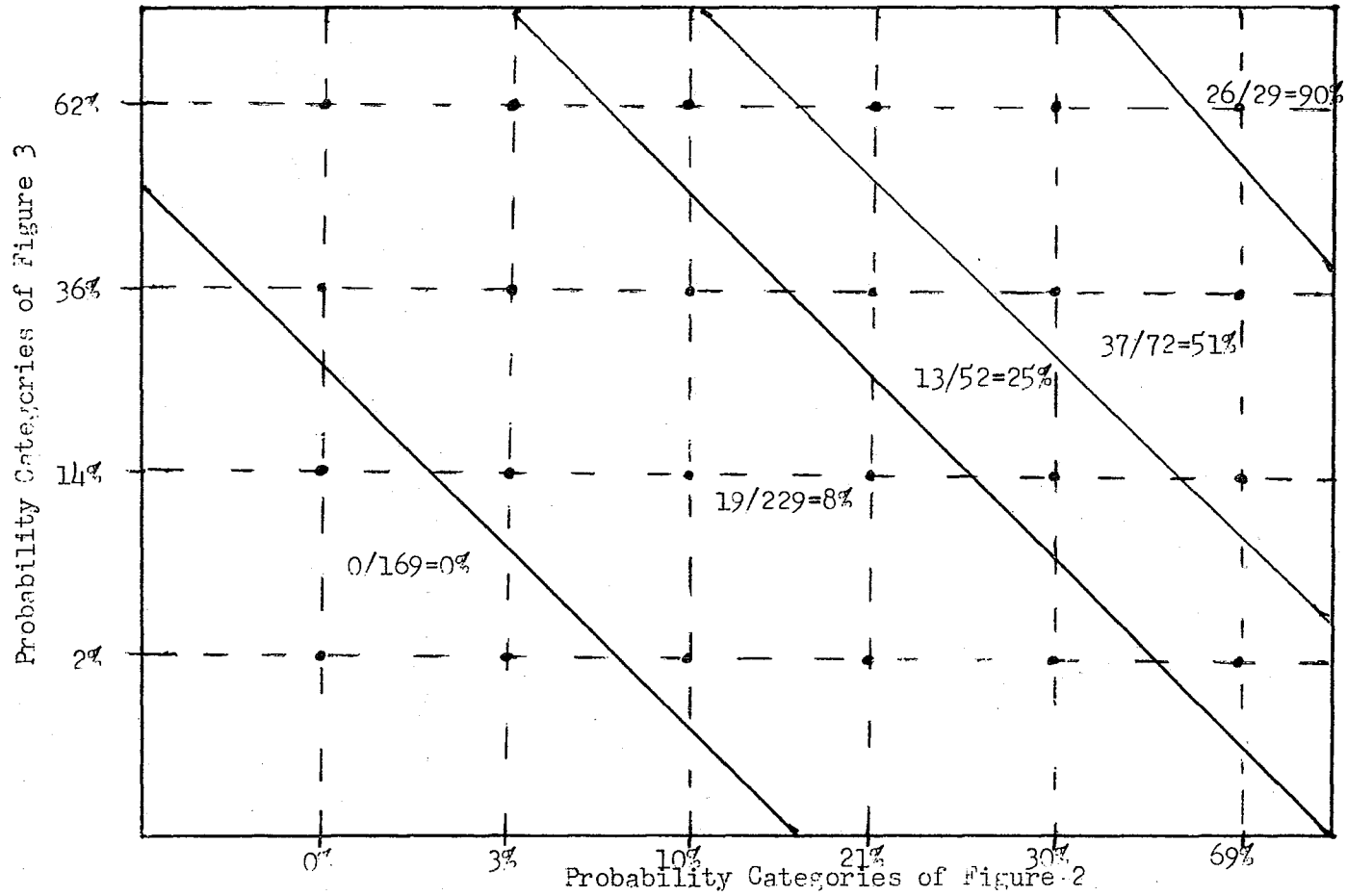


Figure 4. Probability of measurable precipitation as a function of the isoplethed probability categories of Figure 2 versus the probability categories of Figure 3.

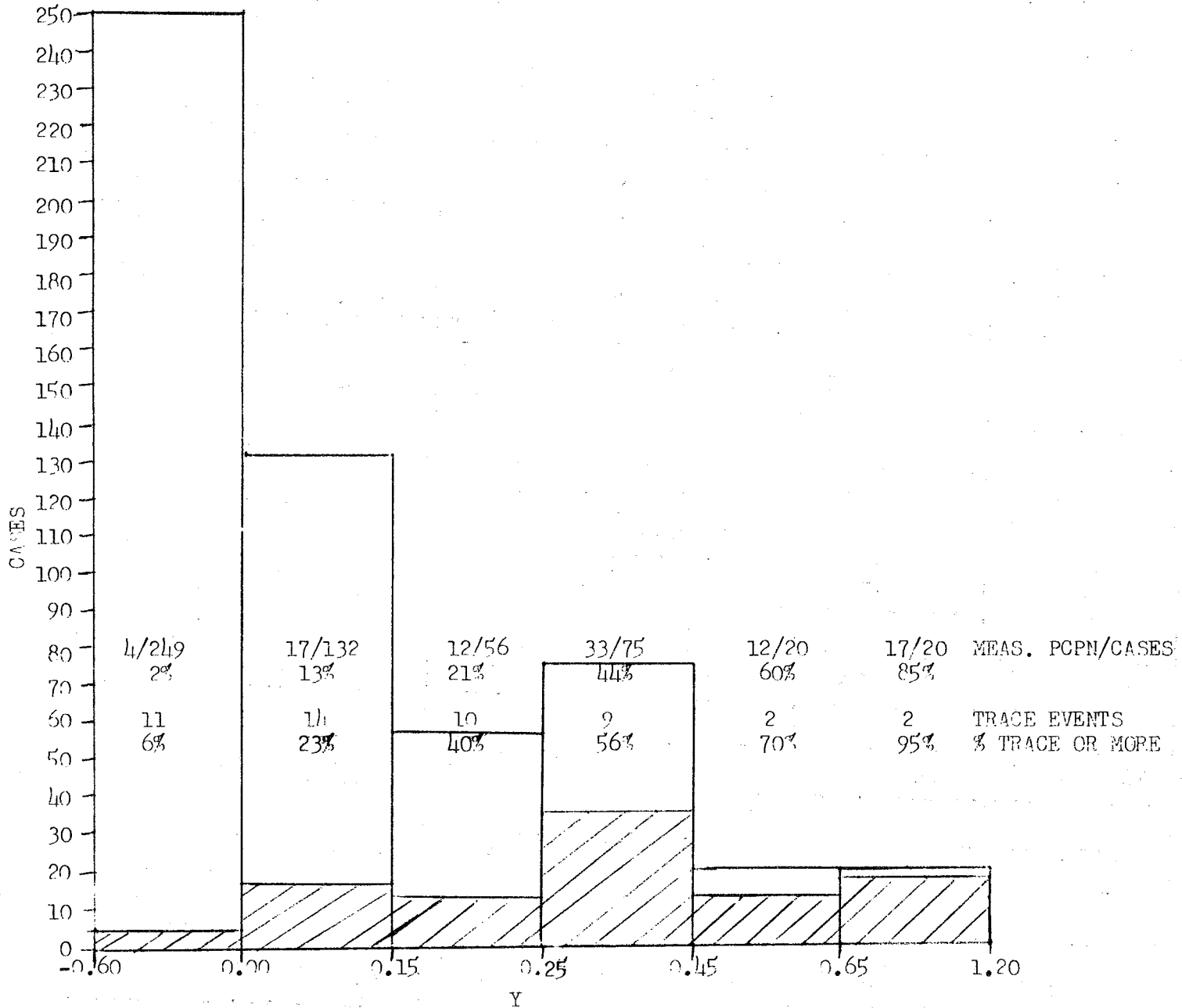


Figure 5. Histogram displaying the range of Y values from the linear regression, $Y = .01251X_1 + .00132X_2 + .02361X_3$, for 551 cases. Measurable precipitation cases are shaded.

GTF 500mb LAT. CONT. CROSSING (C)	115W			130W		
	PCPN/CASES	GTF 500mb CROSSING IN 5 DEG INTERVAL	PCPN/CASES	PCPN/CASES	GTF 500mb CROSSING IN 5 DEG INTERVAL	PCPN/CASES
$\geq 65N$	27/41 = 66%			17/29 = 59%		
		$65 < C \leq 60N$	17/37 = 46%		$65 < C \leq 60N$	21/45 = 47%
$\geq 60N$	48/78 = 56%			38/74 = 51%		
		$60 < C \leq 55N$	10/31 = 32%		$60 < C \leq 55N$	28/79 = 35%
$\geq 55N$	54/109 = 50%			66/153 = 43%		
		$55 < C \leq 50N$	17/75 = 23%		$55 < C \leq 50N$	12/142 = 8%
$\geq 50N$	71/184 = 39%			78/295 = 26%		
		$50 < C \leq 45N$	11/117 = 9%		$50 < C \leq 45N$	12/145 = 8%
$\geq 45N$	82/301 = 27%			90/440 = 20%		
		$45 < C \leq 40N$	8/138 = 6%		$45 < C \leq 40N$	5/91 = 5%
$\geq 40N$	90/439 = 21%			95/531 = 18%		
		$40 < C \leq 35N$	5/102 = 5%		$40 < C \leq 35N$	0/34 = 0%
$\geq 35N$	95/541 = 18%			95/565 = 17%		
		$35 < C \leq 30N$	0/31 = 0%		$35 < C \leq 30N$	0/11 = 0%
$\geq 30N$	95/572 = 17%			95/576 = 16%		
		$30 < C \leq 25N$	0/8 = 0%		$30 < C \leq 25N$	0/4 = 0%
$\geq 25N$	95/580 = 16%			95/580 = 16%		

Table 1. Measurable precipitation probability at GTF as a function of the GTF 500-mb contour crossing at the 115 W and 130 W meridians.

GREAT FALLS 500mb CONTOUR CROSSING(deg latitude)	PCPN/TOTAL PCPN CASES
145W CONTOUR CRSG \geq 130W and 120W CONTOUR CRSGS	57/95 = 60%
130W CONTOUR CRSG $>$ 145W and \geq 120W CONTOUR CRSGS	27/95 = 28%
120W CONTOUR CRSG $>$ 145W and 130W CONTOUR CRSGS	11/95 = 12%

Table 2. A breakdown of all measurable precipitation cases in this study as a function of the highest latitudinal crossing of the GTF 500-mb contour at key longitude meridians.

JANUARY 1977 DATE/TIME	12 HR PRECIP FOLLOWING DATE/TIME (in.)	MOS POP (%)	DERIVED EQUATION POP (%)
03/00Z	TRACE	10	40
03/12Z	.12	30	80
04/00Z	.16	70	80
04/12Z	.07	70	80
05/00Z	.03	30	40
05/12Z	.00	20	20
06/00Z	.00	5	10
06/12Z	.16	0	2
07/00Z	.00	20	10
07/12Z	.07	20	60
08/00Z	.01	20	80
08/12Z	TRACE	30	20
09/00Z	TRACE	10	20
09/12Z	.01	20	40
10/00Z	.00	10	40
10/12Z	.13	20	40
11/00Z	.04	20	20

Table 3. A comparison of MOS and derived-equation first-period probabilities, 3-11 January 1977.

OCTOBER 1977 DATE/TIME	12 HR PRECIP FOLLOWING DATE/TIME (in.)	MOS POP (%)	DERIVED EQUATION POP (%)
22/00Z	0	5	10
22/12Z	0	5	2
23/00Z	0	20	2
23/12Z	0	30	2
24/00Z	0	20	2
24/12Z	0	0	2
25/00Z	0	0	2
25/12Z	0	0	2
26/00Z	TRACE	60	2
26/12Z	TRACE	30	2
27/00Z	0	5	2
27/12Z	0	0	2
28/00Z	0	0	10
28/12Z	0	0	20
29/00Z	0	0	10
29/12Z	0	20	2
30/00Z	0	20	10
30/12Z	0	20	10
31/00Z	0	2	10
31/12Z	0	0	2

Table 4. A comparison of MOS and derived-equation first-period probabilities during a relatively dry period in October 1977.

DEC 1977	12 HR	PROBABILITIES OF PRECIPITATION						
	PRECIP	1st Period		2nd Period		3rd Period		
	AFTER DATE/TIME (in.)	DERIV. EQ (%)	MOS (%)	DERIV. EQ (%)	MOS (%)	DERIV. EQ (%)	MOS (%)	
	3/00Z	0	2	60	10	40	20	40
	3/12Z	0	10	40	2	30	2	30
	4/00Z	TRACE	20	30	20	40	10	30
	4/12Z	.06	40	50	20	40	60	30
	5/00Z	.03	80	70	40	40	40	20
	5/12Z	0	80	20	80	30	60	20
	6/00Z	.03	80	20	80	30	80	30
	6/12Z	.11	80	40	80	60	60	50
	7/00Z	.05	40	50	40	40	60	50
	7/12Z	.01	40	50	40	30	80	30
	8/00Z	TRACE	80	60	60	40	60	30
	8/12Z	0	80	50	80	60	60	30
	9/00Z	.01	80	30	80	40	80	20
	9/12Z	.01	60	20	80	30	80	50
	10/00Z	TRACE	40	20	60	30	80	30
	10/12Z	0	10	30	10	20	60	40
	11/00Z	0	2	0	2	5	2	20
	11/12Z	0	2	0	2	0	2	0
	12/00Z	0	2	2	2	0	2	10
	12/12Z	0	2	10	10	30	2	5
	13/00Z	0	10	2	2	5	2	20
	13/12Z	0	2	10	10	10	2	10
	14/00Z	.01	2	5	2	5	2	20
	14/12Z	TRACE	2	5	2	20	2	10

Table 5. A comparison of MOS and derived equation 1st, 2nd, and 3rd 12-hour period probabilities during a period in December 1977. The data for the derived-equation probabilities were extracted from the 12-, 24-, and 36-hour LFM surface and upper progs.

NOAA Technical Memoranda NWSNR: (Continued)

- 92 Smoke Management in the Willamette Valley. Earl M. Bates, May 1974. (COM-74-11277/AS)
- 93 An Operational Evaluation of 500-mb Type Stratified Regression Equations. Alexander E. MacDonald, June 1974. (COM-74-11407/AS)
- 94 Conditional Probability of Visibility Less than One-Half Mile in Radiation Fog at Fresno, California. John D. Thomas, August 1974. (COM-74-11955/AS)
- 95 Climate of Flagstaff, Arizona. Paul W. Sorenson, August 1974. (COM-74-11678/AS)
- 96 Map Type Precipitation Probabilities for the Western Region. Glenn E. Rasch and Alexander E. MacDonald, February 1975. (COM-75-10428/AS)
- 97 Eastern Pacific Cut-off Low of April 21-23, 1974. William J. Alder and George R. Miller, January 1976. (PB-250-711/AS)
- 98 Study on a Significant Precipitation Episode in the Western United States. Ira S. Brenner, April 1975. (COM-75-10719/AS)
- 99 A Study of Flash Flood Susceptibility--A Basin in Southern Arizona. Gerald Williams, August 1975. (COM-75-11360/AS)
- 100 A Study of Flash-Flood Occurrences at a Site Versus Over a Forecast Zone. Gerald Williams, August 1975. (COM-75-11404/AS)
- 102 A Set of Rules for Forecasting Temperatures in Napa and Sonoma Counties. Wesley L. Tuft, October 1975. (PB-246-902/AS)
- 103 Application of the National Weather Service Flash-Flood Program in the Western Region. Gerald Williams, January 1976. (PB-253-053/AS)
- 104 Objective Aids for Forecasting Minimum Temperatures at Reno, Nevada, During the Summer Months. Christopher D. Hill, January 1976. (PB-252-666/AS)
- 105 Forecasting the Mono Wind. Charles P. Ruscha, Jr., February 1976. (PB-254-650)
- 106 Use of MOS Forecast Parameters in Temperature Forecasting. John C. Plankinton, Jr., March 1976. (PB-254-649)
- 107 Map Types as Aid in Using MOS Maps in Western United States. Ira S. Brenner, August 1976. (PB250594)
- 108 Other Kinds of Wind Shear. Christopher D. Hill, August 1976. (PB250437/AS)
- 109 Forecasting North Winds in the Upper Sacramento Valley and Adjoining Forests. Christopher E. Fontana, September 1976.
- 110 Cool Inflow as a Weakening Influence on Eastern Pacific Tropical Cyclones. William J. Denney, November 1976. (PB 264655/AS)
- 111 Operational Forecasting Using Automated Guidance. Leonard W. Snellman, February 1977. (PB 273663/AS) Out of print.
- 112 The MAN/MOS Program. Alexander E. MacDonald, February 1977. (PB 265941/AS)
- 113 Winter Season Minimum Temperature Formula for Bakersfield, California, Using Multiple Regression. Michael J. Gard, February 1977. (PB 273694/AS)
- 114 Tropical Cyclone Kathleen. James R. Fors, February 1977. (PB 273676/AS)
- 115 Program to Calculate Winds Aloft Using a Hewlett-Packard 25 Hand Calculator. Brian Finke, February 1977. (Out of print)
- 116 A Study of Wind Gusts on Lake Mead. Bradley Colman, April 1977. (PB 268847)
- 117 The Relative Frequency of Cumulonimbus Clouds at the Nevada Test Site as a Function of K-value. R. F. Quiring, April 1977. (PB 272631)
- 118 Moisture Distribution Modification by Upward Vertical Motion. Ira S. Brenner, April 1977. (PB 265740)
- 119 Relative Frequency of Occurrence of Warm Season Echo Activity as a Function of Stability Indices Computed from the Yucca Flat, Nevada, Rawinsonde. Darryl Renserson, June 1977. (PB 271200/AS)
- 120 Some Meteorological Aspects of Air Pollution in Utah with Emphasis on the Salt Lake Valley. Dean N. Jackman and William T. Chapman, June 1977. (PB 271267/AS)
- 121 Climatological Prediction of Cumulonimbus Clouds in the Vicinity of the Yucca Flat Weather Station. R. F. Quiring, June 1977. (PB 271704/AS)
- 122 A Method for Transforming Temperature Distribution to Normality. Morris S. Webb, Jr., June 1977. (PB 271742/AS)
- 123 Study of a Heavy Precipitation Occurrence in Redding, California. Christopher E. Fontana, June 1977. (PB 273624/AS)
- 124 Statistical Guidance for Prediction of Eastern North Pacific Tropical Cyclone Motion - Part I. Charles J. Neumann and Preston W. Leftwich, August 1977. (PB 272661)
- 125 Statistical Guidance on the Prediction of Eastern North Pacific Tropical Cyclone Motion - Part II. Preston W. Leftwich and Charles J. Neumann, August 1977. (PB 273155/AS)
- 126 Climate of San Francisco. E. Jan Null, March 1978.

NOAA SCIENTIFIC AND TECHNICAL PUBLICATIONS

NOAA, the *National Oceanic and Atmospheric Administration*, was established as part of the Department of Commerce on October 3, 1970. The mission responsibilities of NOAA are to monitor and predict the state of the solid Earth, the oceans and their living resources, the atmosphere, and the space environment of the Earth, and to assess the socioeconomic impact of natural and technological changes in the environment.

The six Major Line Components of NOAA regularly produce various types of scientific and technical information in the following kinds of publications:

PROFESSIONAL PAPERS—Important definitive research results, major techniques, and special investigations.

TECHNICAL REPORTS—Journal quality with extensive details, mathematical developments, or data listings.

TECHNICAL MEMORANDUMS—Reports of preliminary, partial, or negative research or technology results, interim instructions, and the like.

CONTRACT AND GRANT REPORTS—Reports prepared by contractors or grantees under NOAA sponsorship.

TECHNICAL SERVICE PUBLICATIONS—These are publications containing data, observations, instructions, etc. A partial listing: Data serials; Prediction and outlook periodicals; Technical manuals, training papers, planning reports, and information serials; and Miscellaneous technical publications.

ATLAS—Analysed data generally presented in the form of maps showing distribution of rainfall, chemical and physical conditions of oceans and atmosphere, distribution of fishes and marine mammals, ionospheric conditions, etc.



Information on availability of NOAA publications can be obtained from:

**ENVIRONMENTAL SCIENCE INFORMATION CENTER
ENVIRONMENTAL DATA SERVICE
NATIONAL OCEANIC AND ATMOSPHERIC ADMINISTRATION
U.S. DEPARTMENT OF COMMERCE**

**3300 Whitehaven Street, N.W.
Washington, D.C. 20235**